NEOPLASIA
www.neoplasia.com

Volume 17 Number 5 May 2015 pp. 449–462 449

# STAT1: A Novel Target of miR-150 and miR-223 Is Involved in the Proliferation of HTLV-I–Transformed and ATL Cells[1]

**Ramona Moles, Marcia Bellon and Christophe Nicot**

Department of Pathology and Laboratory Medicine, University of Kansas Medical Center, Kansas City, KS, USA

## Abstract

We have previously reported on the deregulation of cellular microRNAs involved in hematopoiesis and inflammation in human T-cell lymphotropic virus type 1 (HTLV-I)–transformed cells. In this study, we demonstrate that miR-150 and miR-223 specifically target the signal transducer and activator of transcription 1 (STAT1) 3′ untranslated region, reducing STAT1 expression and dampening STAT1-dependent signaling in human T cells. The effects of miR-150 and miR-223 on endogenous STAT1 were confirmed using inducible cell lines. Our studies also showed that miR-150 expression is upregulated by interleukin-2 signaling in adult T cell leukemia/lymphoma (ATL) cells. HTLV-I–transformed and ATL-derived cells have reduced levels of miR150 and miR223 expression, which coincide with increased STAT1 expression and STAT1-dependent signaling. Knockdown of STAT1 by short hairpin RNA demonstrated that the constitutive activation of STAT1 is required for the continuous proliferation of HTLV-I–transformed cells. Our studies further demonstrate that increased expression of STAT1 in ATL cells is associated with higher levels of major histocompatibility complex class I expression. Previous studies have demonstrated that the pressure exerted by natural killer (NK) cells *in vivo* can edit leukemic tumor cells by forcing an increased expression of major histocompatibility complex class I to escape immune clearance. STAT1-expressing tumor cells produce more aggressive tumors because they cannot be eliminated by NK cells. Our results suggest that therapeutic approaches using combined targeting of STAT1 and MHC class I may be an effective approach to activate NK cell–mediated clearance of ATL tumor cells.

*Neoplasia (2015) 17, 449–462*

## Introduction

MicroRNAs (miRNAs) are involved in a wide range of biologic processes, including cellular survival, differentiation, immune response, and oncogenesis. miRNAs are short non-coding RNAs that target genes through imperfect base pairing with mRNAs, thereby affecting their stability and/or their translation. An individual miRNA has numerous cellular gene targets and the manner in which to accomplish a coordinated regulation of biologic processes is unclear. The role of miR-150 in human cancer is context-dependent as this miRNA can have either oncogenic or tumor suppressor activity in cells that originate from different tissues. This is best illustrated by upregulated expression of miR-150 in CD19+ B cells from chronic lymphocytic leukemia (CLL) [1,2] but downregulated expression in chronic myeloid leukemia [3,4], acute lymphoblastic leukemia [5], and mantle cell lymphoma [6]. Additional studies have further demonstrated that miR-150 stimulates the proliferation and migration of lung cancer cells by targeting SRC kinase signaling inhibitor 1 (SRCIN1) and SRC activity [7]. In contrast, *in situ* hybridization revealed that miR-150 expression levels are reduced in both estrogen receptors positive and triple-negative breast cancer samples compared to adjacent normal cells, and miR-150 expression was shown to inhibit breast cancer cell migration and invasion [8,9]. Some of the known validated cellular gene targets of miR-150 include c-MYB, NOTCH3, CBL, EGR2, AKT2, and DKC1

Address all correspondence to: C. Nicot, PhD, Department of Pathology and Laboratory Medicine, University of Kansas Medical Center, 3901 Rainbow Boulevard, Kansas City, KS 66160, USA.
E-mail: cnicot@kumc.edu

[1] Adult T cell leukemia/lymphoma (ATL)–derived cells MT-1, TL-Om1, and ED-40515(–) were provided by Michiyuki Maeda. ATL-derived cells ATL-43T, ATL-55T, ATL-25, and ATL-T were provided by Masao Matsuoka. ATL-derived cell LMY1 was provided by Hiroo Hasegawa. This work was supported by a grant from the National Cancer Institute (CA141386) to C.N.
Received 31 December 2014; Revised 13 April 2015; Accepted 24 April 2015


1476-5586
http://dx.doi.org/10.1016/j.neo.2015.04.005

**Table 1.** Predicted miRNA Target Sites of Human STAT1

| miRNAs | Total Sites | 8mer | 7mer-m8 | 7mer-1A | Aggregate Probability of Conserved Targeting |
|---|---|---|---|---|---|
| miR-223 | 2 | 1 | 0 | 1 | 0.27 |
| miR-150 | 1 | 0 | 0 | 1 | 0.14 |
| miR-144 | 1 | 1 | 0 | 0 | <0.1 |
| miR-130ac | 1 | 0 | 0 | 1 | <0.1 |
| miR-155 | 1 | 0 | 0 | 1 | <0.1 |
| miR-140 | 1 | 0 | 1 | 0 | <0.1 |
| miR-203 | 1 | 1 | 0 | 0 | <0.1 |
| miR-27abc | 1 | 0 | 0 | 1 | <0.1 |
| miR-200bc | 1 | 0 | 0 | 1 | <0.1 |
| miR-101 | 1 | 0 | 0 | 1 | <0.1 |
| miR-146ac | 1 | 0 | 1 | 0 | <0.1 |
| miR-132 | 1 | 0 | 0 | 1 | <0.1 |
| miR-26ab | 1 | 0 | 0 | 1 | <0.1 |

[10–14]. Similar to miR-150, miR-223 is also differentially regulated. Studies showed that it is frequently repressed in hepatocellular carcinoma [15], B-CLL [16], acute myeloid leukemia (AML) [17], gastric mucosa-associated lymphoid tissue lymphoma [18], and recurrent ovarian cancer [19]. In contrast, miR-223 is upregulated in T cell acute lymphocytic leukemia (T-ALL) [20], EBV-positive diffuse large B-cell lymphoma [21], and metastatic gastric cancer [22,23]. Among validated cellular gene targets of miR-223 are FBXW7/Cdc4, RhoB, stathmin 1, E2F transcription factor 1 (E2F1), signal transducer and activator of transcription 3 (STAT3), CCAAT/enhancer binding protein beta, forkhead box O1, and nuclear factor I/A [22–27].

Human T-cell lymphotropic virus type 1 (HTLV-I) is a human retrovirus present in 20 million people worldwide [28]. Infection with HTLV-I is the etiological agent of adult T cell leukemia/lymphoma (ATL) [29] and a neurodegenerative disease called tropical spastic paraparesis/HTLV-I–associated myelopathy [30,31]. Only a few studies have investigated miRNA expression in HTLV-I–mediated T cell transformation and pathogenesis [32–37]. HTLV-I–associated disease pathogenesis is still poorly understood [38–40]. Both diseases originate from deregulated proliferation of infected CD4/CD25+ T cells. While it is unclear how the virus induces cellular transformation, the viral oncoprotein Tax plays an essential role and is sufficient to immortalize human primary T cells [41]. Tax expression leads to accumulation of DNA double-strand breaks during cellular replication and simultaneously targets DNA repair pathways to increase genetic instability [42,43]. In addition, Tax targets many tumor suppressors, cell cycle regulators, and survival factors and affects chromosome stability and segregation [44–48]. The molecular events linked to the switch from immortalization [interleukin-2 (IL-2)–dependent growth] to transformation (IL-2–independent growth) are largely unknown. A common characteristic found in HTLV-I–transformed cells *in vivo* and *in vitro* is the constitutive activation of the Janus activated kinase (JAK)/STAT signaling [49,50]. In fact, pharmacological targeting of the JAK/STAT axis has shown that activation of this pathway is required for continuous proliferation and survival of HTLV-I–transformed cells [51–53]. STAT1 plays a role in immune modulatory functions, anti-viral responses, apoptosis, and anti-proliferative responses [54]. In contrast, several studies have shown that STAT1 can also act as a potent tumor promoter for leukemia development [55] and that many T-ALL leukemic cells are dependent on the TYK2-STAT1-BCL2 pathway for continued survival [56]. However, a potential role played by STAT1 in HTLV-I pathogenesis has not yet been investigated.

In this study, we demonstrate for the first time that miRNAs miR-150 and miR-223 directly target the STAT1 3′ untranslated region (UTR) gene. Expression of both miR-150 and miR-223 was significantly reduced in HTLV-I–transformed cell lines and ATL-derived cells, while STAT1 protein expression was elevated. Restoring miR-150 and miR-223 expression inhibited endogenous STAT1 expression and the activation of STAT1 transcription–dependent genes and significantly reduced the proliferation of HTLV-I–transformed cells and ATL cells. A direct role of STAT1 on cell cycle and expansion of HTLV-I cells was further confirmed by using short hairpin RNA (shRNA) targeting STAT1. We also found that IL-2–dependent ATL cell lines express higher levels of miR-150, suggesting that IL-2 signaling may be involved in the transcriptional up-regulation of miR-150 expression. Finally, we found that a majority of freshly isolated uncultured ATL samples have high expression of STAT1, which correlated with higher major histocompatibility complex class I (MHC-I) expression and may help to conceal ATL cells against immune clearance by natural killer (NK) cells.

## Experimental Procedure

### *miRNA Target Predictions*

STAT1 sequences were obtained from the National Center for Biotechnology Information Nucleotide database (http://www.ncbi.nlm.nih.gov/). Sequences of mature human miRNAs were obtained from the miRNA Registry at miRBase (http://www.mirbase.org). The prediction algorithms Targetscan and PicTar were used to search for miRNA target sites in the human STAT1 3′UTR.

### *Cell Culture and Patient Samples*

A 293T cell line was cultured in complete Dulbecco's modified Eagle's medium with 10% FBS, penicillin, and streptomycin. The HTLV-I cell lines, MT-4, MT-2, C8166, C91PL, and human T cell lymphoblast cell line, Jurkat, were maintained in RPMI-1640 (Invitrogen, Carlsbad, CA) supplemented with 10% FBS, penicillin, and streptomycin. The ATL-like cell lines, MT-1, ATL-T, ED-40515(-), ALT-25, ATL-43T, LMY1, and ATL-55T, were maintained in RPMI-1640 supplemented with 10% FBS, penicillin, and streptomycin and IL-2 (50 U/ml) as needed [57–59]. Patient samples were obtained after informed consent was provided and in agreement with regulations for the protection of human subjects according to the National Institutes of Health guidelines. RNA was extracted from peripheral blood mononuclear cells (PBMCs) of patients with acute ATL and healthy donors (HD). RNA was extracted from PBMCs of patients with ATL.

### *Plasmids*

Precursors of miR-150 and miR-223 were cloned in pTRIPZ. pTRIPZ lentivirus is an inducible vector engineered to be Tet-On.

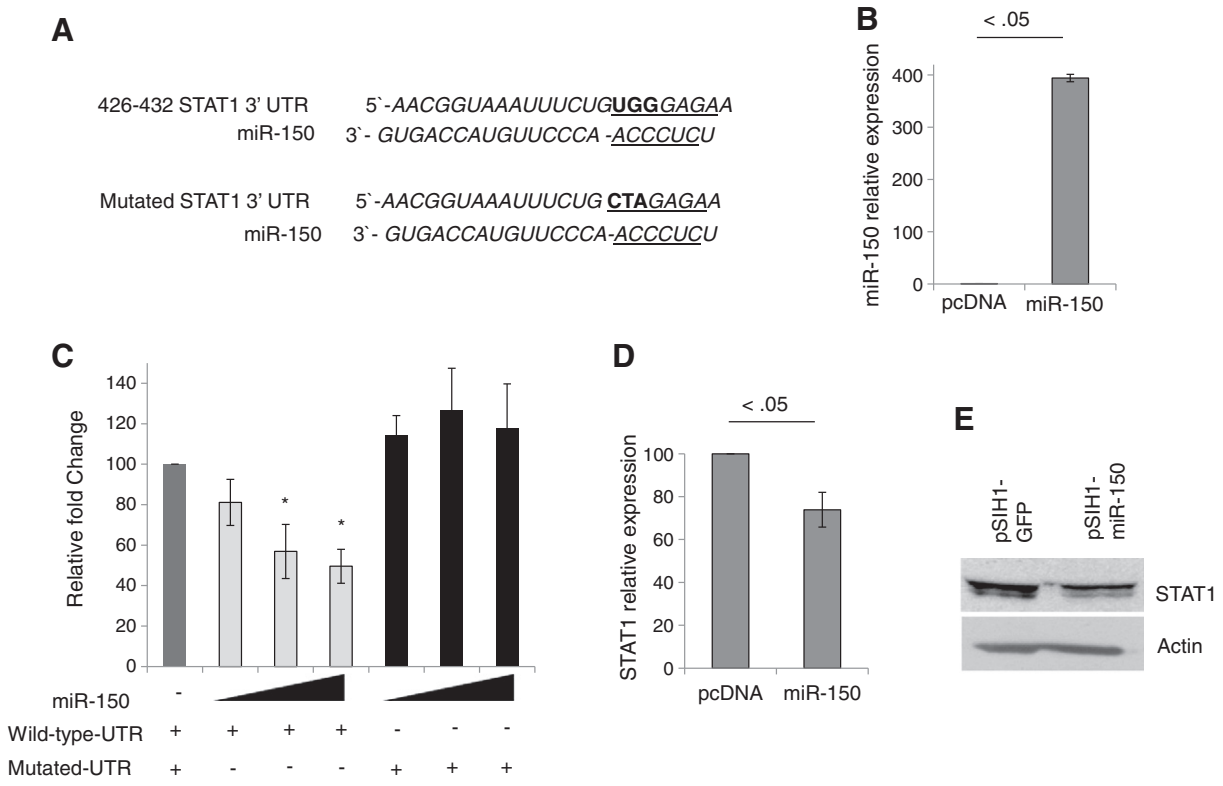


**Figure 1.** STAT1 is a direct target of miRNA miR-150. (A) A diagram representing the sequence alignment of miR-150 and its target site within STAT1 3′UTR and the relative mutated version. The mutations made in the STAT1 3′UTR are highlighted. (B) Real-time PCR was performed on mature miR-150 from cDNA derived from 293T cells transfected with pcDNA or miR-150. Real-time PCR was performed in duplicate, and samples were normalized to RNU6b (U6) expression. (C) 293T cells were cotransfected with wild-type (or mutated) STAT1 3′UTR luciferase reporter plasmids and pTK–Renilla luciferase plasmids, together with a control plasmid (pcDNA) or a different amount of miR-150 (0.125, 0.25, 0.75 μg). After 48 hours, firefly luciferase activity was measured and normalized by Renilla luciferase activity. The data are representative from two independent experiments. (D) Real-time PCR of STAT1 expression was performed from total cDNA from 293T cells transfected with pcDNA or miR-150 (2 μg). Extracts were analyzed 48 hours after transfection and normalized to GAPDH expression. *P* value was <.05. (E) Western blot analysis of STAT1 expression from total cellular extracts of 293T cells infected with lentivirus expressing miR-150 or empty lentivirus used as a control. Extracts were normalized to actin expression. Semiquantitative analysis of Western blot data demonstrated 24.9% inhibition of STAT1 expression by miR-150. Western blot quantification was performed by using the Java-based image processing program ImageJ.

pTRIPZ contains puromycin resistance that was used to select a stable cell line. The stable cell lines derived were incubated in the absence or presence of doxycycline and subjected to reverse transcription–polymerase chain reaction (RT-PCR) to analyze miR-150 and miR-223 expression. Precursors of miR-150 and miR-223 were also cloned in the pSIH1-green fluorescent protein (GFP) lentivirus and pcDNA vector. shRNA against STAT1 was cloned in the pSIH1-GFP vector.

### *3′UTR and Luciferase Reporter Assay*

The full-length 3′UTR of the human *STAT1* gene was cloned into the luciferase vector, pGL3 (Promega). STAT1 3′UTR containing the mutated miR-150 target sequence and the mutated miR-223 target sequence were generated by QuikChange Site-Directed Mutagenesis kit (Stratagene). miR-150 and miR-223 were cloned into the pcDNA expression vector. 293T cells were cotransfected using Polyfect Transfection reagent (Qiagen), with 300 ng of the indicated luciferase reporter plasmid, 200 ng of pRL-TK–Renilla luciferase plasmid (Promega, for normalization), and the indicated miRNAs (125, 250, 500, or 750 ng). Cell extracts were prepared 48 hours after transfection. Cell extracts were lysed in 1× passive lysis buffer (Promega) and analyzed using the Luciferase Reporter Assay System (Promega), according to the manufacturer's instructions. Luciferase assays were performed twice from independent experiments, and data were normalized for transfection efficiency using Renilla luciferase activity. 293T cells were cotransfected with 300 ng of the STAT1 luciferase reporter plasmid, 200 ng of pRL-TK–Renilla luciferase, and the indicated miRNAs. Cell extracts were prepared 48 hours after transfection according to the manufacturer's instructions.

293T cells were stimulated with 500 pg/ml human interferon-γ (IFN-γ; PBL Assay Science, Piscataway, NJ) or 100 U/ml human IFN-β (ProSpec, East Brunswick, NJ) and cotransfected with 300 ng of pISRE-TA-Luc Vector, 200 ng of pRL-TK–Renilla luciferase plasmid, and 500 ng of the indicated miRNAs by using Polyfect. Cell extracts were prepared 48 hours after transfection and luciferase assays were performed as described above.

### *Transfection, Viruses, and Generation of Stable miR-150 and miR-223 Inducible Cell Lines*

293T cells were infected with lentiviral particles expressing miR-150 and miR-223. Lentiviruses were prepared by transfection of 293T cells with 10 μg of pSIH1-miR-150, pSIH1-miR-223,

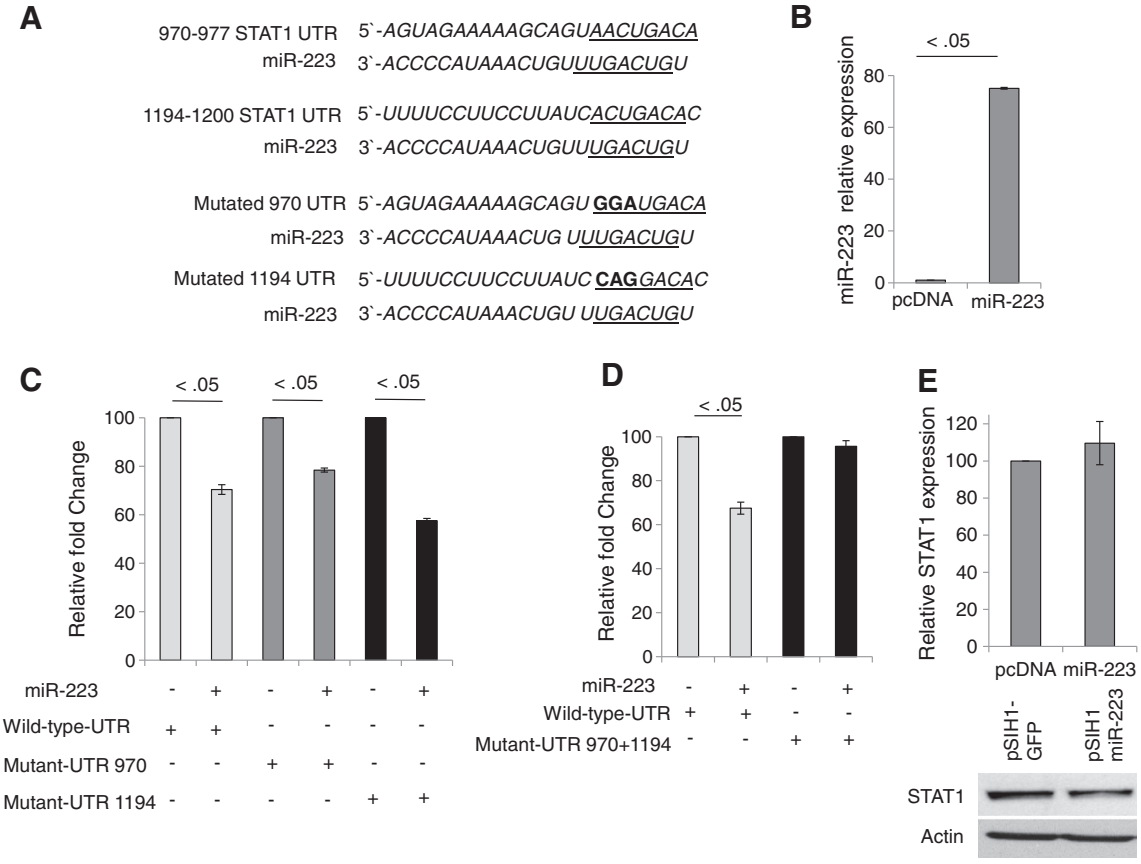


**Figure 2.** STAT1 is a direct target of miRNA miR-223. (A) The diagrams represent the sequence alignment of miR-223 and its target sites within the STAT1 3′UTR and the relative mutated versions. The mutations made in the STAT1 3′UTR are highlighted. (B) Real-time PCR was performed on mature miR-223 from cDNA derived from 293T cells transfected with pcDNA or miR-223. Real-time PCR was performed in duplicate, and samples were normalized to RNU6b (U6) expression. (C, D) 293T cells were cotransfected with wild-type (or mutated) STAT1 3′UTR firefly luciferase reporter plasmids and pTK–Renilla luciferase plasmids, together with a control plasmid (pcDNA) or miR-223. After 48 hours, firefly luciferase activity was measured and normalized to Renilla luciferase activity. The data are representative from two independent experiments. (E) Real-time PCR of STAT1 expression was performed from total cDNA from 293T cells transfected with pcDNA or miR-223 (2 $\mu$g). Extracts were analyzed 48 hours after transfection and normalized to GAPDH expression. Western blot analysis of STAT1 expression from total cellular extracts of 293T cells infected with lentivirus expressing miR-223 or empty lentivirus used as a control is also shown. Extracts were normalized to actin expression. miR-223 demonstrated a 38.1% inhibition of STAT1 expression. Western blot quantification was performed by using the Java-based image processing program ImageJ.

pTRIPz/miR-150, or pTRIPz/miR-223, 5 μg of vesicular stomatitis virus G proteins, and 5 μg of pDNL6 using calcium phosphate (Invitrogen). The virus was collected in the supernatant for 4 days, concentrated by ultracentrifugation, and resuspended in phosphate-buffered saline. For inducible miR-150 and miR-223 expression assays, MT-4 or Jurkat cells were infected with lentiviruses encoding vector control (pTRIPz), miR-150 (pTRIPz/miR-150), or miR-223 (pTRIPz/miR-223). Cells were selected with 10 μg/ml puromycin for 12 days. Stable cell lines derived were incubated in the absence or presence of doxycycline and subjected to RT-PCR to analyze miR-150 and miR-223 expression.

### *RNA Extraction and Real-Time Quantitative PCR*

RNA was extracted using TRIzol (Invitrogen) and treated with DNaseI (Roche Applied Science, Indianapolis, IN). RNA was reverse-transcribed using the RNA-to-cDNA synthesis kit (Applied Biosystems, Carlsbad, CA). Quantitative real-time PCR was performed using Real-Time SYBR Green PCR Master Mix (SABiosciences, Valencia, CA) on the StepOnePlus Real-Time PCR System (Applied Biosystems), with glyceraldehyde-3-phosphate dehydrogenase (GAPDH) expression as an internal control. The miScript II RT Kit was used for mature miRNA quantification. cDNA generated with the miScript II RT Kit was used as a template for real-time PCR to detect the expressive level of mature miR-150 and miR-223 in HTLV-I and ATL cell lines. Real-time PCR was performed in duplicate, and samples were normalized to RNU6b (U6) expression.

### *Western Blot Analysis*

Cells were washed with phosphate-buffered saline and lysed in RIPA buffer with phosphatase and protease inhibitors (Complete Cocktail; Roche). Protein concentration was determined with the Bio-Rad protein assay (Bio-Rad, Hercules, CA). Total protein extracts were resolved by sodium dodecyl sulfate–polyacrylamide gel electrophoresis, transferred to Immobilon polyvinylidene difluoride membranes (Millipore, Darmstadt, Germany), and probed with

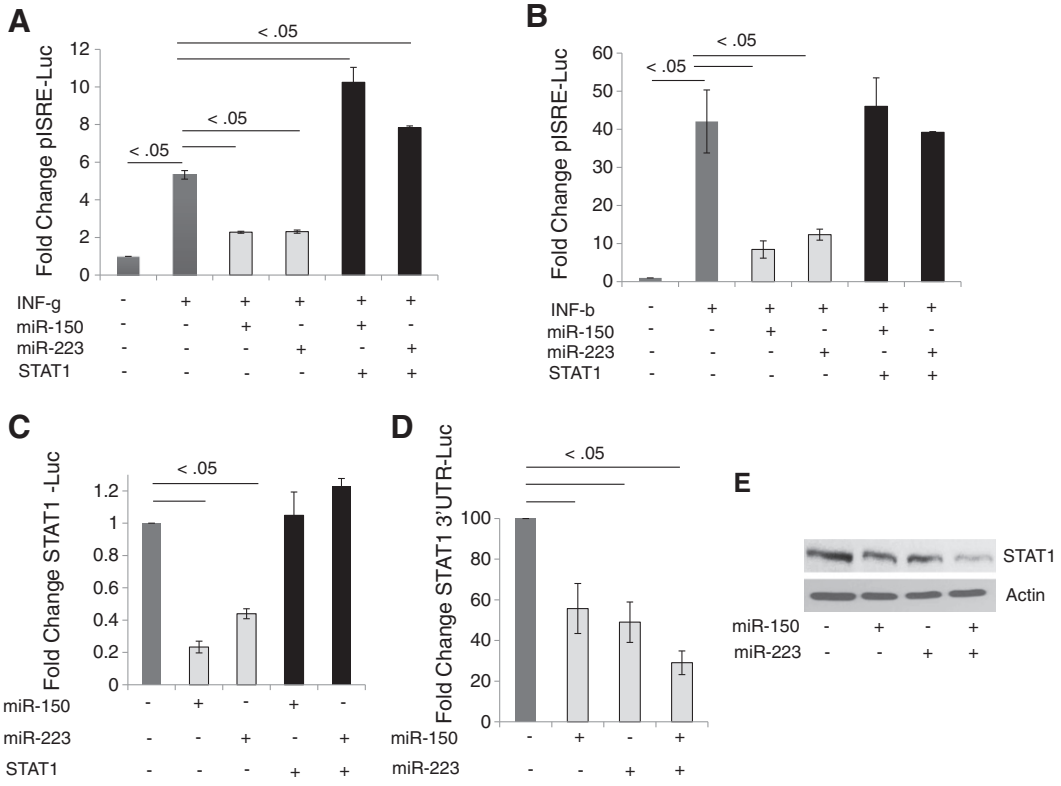


**Figure 3.** miR-150 and miR-223 hamper the IFN-mediated response by inhibition of STAT1 activity. (A) 293T cells stimulated with 500 pg/ml human IFN-γ and co-transfected with the pISRE firefly luciferase reporter plasmid and pTK–Renilla luciferase plasmid, together with a control plasmid (pcDNA), miR-150, miR-223, and/or STAT1 cDNA expressing vector lacking the 3′UTR sequence. After 48 hours, firefly luciferase activity was measured and normalized by Renilla luciferase activity. The data are representative from two independent experiments. (B) 293T cells stimulated with 100U/ml human IFN-β and co-transfected with the pISRE firefly luciferase reporter plasmid and pTK–Renilla luciferase plasmid, together with a control plasmid (pcDNA), miR-150, miR-223, and/or STAT1 cDNA expressing vector lacking the 3′UTR sequence. After 48 hours, firefly luciferase activity was measured and normalized by Renilla luciferase activity. The data are representative from two independent experiments. (C) 293T cells were cotransfected with STAT1-luciferase reporter plasmid and pTK–Renilla luciferase plasmid, together with a control plasmid (pcDNA), miR-150, miR-223, or STAT1 cDNA expressing vector. (D) 293T cells were cotransfected with wild-type STAT1 3′UTR firefly luciferase reporter plasmid and pTK–Renilla luciferase plasmids, together with a control plasmid (pcDNA), miR-150, and/or miR-223. After 48 hours, firefly luciferase activity was measured and normalized by Renilla luciferase activity. (E) 293T cells transfected with pcDNA, mir-150, and/or mir-223 (1 $\mu$g) and 50 ng of pSIH1-puromycin. Forty-eight hours after transfection, the cells were treated with puromycin (1 $\mu$g/ml) for 7 days. Western blot analyses of STAT1 expression from total cellular extracts were performed. Extracts were normalized to actin expression. Semiquantitative analysis of Western blot data shows 9.7% and 9% inhibition of STAT1 expression by mir-150 and mir-223, respectively, compared to the control. Co-transfection of mir-150 and mir-223 demonstrate 23% inhibition of STAT1 expression. Western blot quantification was performed by using the Java-based image processing program ImageJ.

STAT1 (Cell Signaling Technology, Danvers, MA) and Bcl2, p21, p27, or actin (Santa Cruz Biotechnology, Santa Cruz, CA) antibodies. Western blot quantification was performed by using the Java-based image processing program ImageJ (http://imagej.nih.gov/ij/).

## Results

### *miRNAs miR-150 and miR-223 Target the STAT1 3′UTR*

The prediction algorithms Targetscan and PicTar were used to identify common gene targets to miRNAs downregulated in HTLV-I–transformed cells. Among potential targets, STAT1 appeared as a possible target and was selected for further analyses (Table 1). We identified a 7-mer-1A binding site for miR-150 in position 426-432nt of the STAT1 3′UTR (Figure 1*A*). To demonstrate a direct effect of miR-150 on STAT1 mRNA, the full-length (1667 bp) STAT1 3′UTR was cloned into a pGL-3 reporter luciferase construct and miR-150 was cloned into the pcDNA expression vector. First, we verified the transfection of the mature miR-150 by using RT-PCR (Figure 1*B*). Expression of the STAT1 3′UTR vector along with a different amount of miR-150 demonstrated a 50% inhibition of luciferase activity (Figure 1*C*). To further demonstrate specificity, we performed site-directed mutagenesis to modify the seed sequence and generate a mutated STAT1 3′ UTR vector (Figure 1*A*). As expected, miR-150 had no significant effect on the mutated STAT1 3′UTR construct (Figure 1*C*). These results demonstrated a specific and direct effect of miR-150 on the STAT1 3′UTR. We next wanted to validate these results on the endogenous *STAT1* gene. To this end, we expressed in 293T cells the pSIH1-miR-150 or pSIH1-GFP control vector. Our results confirmed the effect of miR-150 on the endogenous *STAT1* gene at both the RNA and the protein levels (Figure 1, *D* and *E*). The down-regulation was not as efficient as seen with the 3′UTR luciferase experiment because in the latter experiment the transfection efficiency limits the percentage of cells in which an effect can be

observed. We then investigated the effect of miR-223. The STAT1 3′ UTR sequence displays two miR-223 target sites positioned at 970-977nt and 1194-1200nt (Figure 2*A*). We verified the transfection of the mature miR-223 by using RT-PCR (Figure 2*B*). To investigate if one site was more important than the other, we mutagenized each site independently (mutant-UTR 970 and mutant-UTR 1194; Figure 2*A*). These mutants were tested along with wild-type STAT1 3′UTR in transient assays. Results indicated that mutation of a single site had no effect and miR-223 was still able to repress activity from the STAT1 3′ UTR (Figure 2*C*). However, when both sites were simultaneously mutated, miR-223 was no longer able to suppress the activity of the STAT1 3′UTR, suggesting that the effect of miR-223 is specific and requires only one functional binding site (Figure 2*D*). We next validated these results on the endogenous *STAT1* gene. We expressed in 293T cells the pSIH1-miR-223 or pSIH1-GFP control vector and analyzed by RT-PCR and Western blot. Results confirmed the effect of miR-223 on the endogenous *STAT1* gene, which was observed at the protein level (Figure 2*E*). RT-PCR analysis shows no significant change in STAT1 expression (Figure 2*E*). That result suggested that miR-223 regulated STAT1 expression at a post-transcriptional level.

### *miR-150 and miR-223 Decrease STAT1 Protein Expression and STAT1 Signaling*

STAT1 is a transcription factor involved in inflammation and cancer. STAT1 is a central mediator of the IFN responses involved in antiviral and immune defense [60]. Since miR-150 and miR-223 target STAT1, we hypothesized that these miRNAs may hamper the IFN-mediated response by dampening STAT1 activity. To test this hypothesis, we first used the ISRE reporter construct plasmid containing four tandem repeats of the IFN-inducible response element. As expected, IFN-γ and IFN-β treatment resulted in the induction of ISRE-luciferase reporter gene activity. Expression of either miR-150 or miR-223 resulted in significant inhibition, which was efficiently rescued by co-expression of a STAT1 cDNA expression vector lacking the 3′UTR sequence (Figure 3, *A* and *B*). IFN-independent, STAT1-dependent signaling was also inhibited by miR-150 and miR-223 as demonstrated by a reduction in STAT1-luciferase reporter construct activity when transfected along with miR-150 or miR-223, which was efficiently rescued by co-expression of a STAT1 cDNA expression vector lacking the 3′ UTR sequence (Figure 3*C*). An additive effect of miR-150 and miR-223 was demonstrated in transient transfection inhibition of the STAT1-3′UTR construct (Figure 3*D*). Finally, Western blot analysis demonstrated that STAT1 expression is reduced more efficiently by the co-transfection of miR-150 and miR-223 (Figure 3*E*).

### *miR-150 and miR-223 Expression Is Inversely Correlated With STAT1 Expression in HTLV-I–Transformed and ATL Cell Lines*

We next investigated the expression of miR-150 and miR-223 in relation to STAT1 in HTLV-I–transformed cell lines (MT-4, MT-2, and C8166). Jurkat cells were used as a negative control since Jurkat cells are human T cells not transformed with HTLV-I. In HTLV-I–transformed cell lines, the expression of both miR-150 and miR-223 was significantly reduced when compared to Jurkat cells (Figure 4*A*). In contrast, the expression of STAT1 was increased at both the RNA and the protein levels (Figure 4, *B* and *C*). We then investigated if such a correlation could also be found in ATL-derived cell lines (MT-1, ATL-T, ED-40515(–), ATL-25). Results from these studies confirmed that both miRNAs, miR-150 and miR-223, were significantly downregulated when compared to Jurkat cells (Figure 4*D*). Consistent with the above data, STAT1 RNA and protein expression was also increased in ATL cells (Figure 4, *E* and *F*). These results suggest an inverse correlation between miR-150 or miR-223 and STAT1 expression in HTLV-I–transformed and ATL-derived cells *in vitro*. Surprisingly, we found that IL-2–dependent ATL-derived cells (ATL-43T and ATL-55T) displayed elevated levels of miR-150 but not miR-223 (Figure 4*G*), suggesting that the former may be regulated through the IL-2 signaling pathway. To further investigate this possibility, we withdrew the IL-2 from the culture media of ATL–IL-2–dependent cells and analyzed the expression of miR-150 after 48 hours. Our results suggest that the absence of IL-2 signaling in ATL cells may be associated with decreased expression of

**Figure 4.** miR-150 and miR-223 expression correlates with STAT1 expression in HTLV-I and ATL cell lines. (A, D) Real-time PCR was performed on mature miR-150 and miR-223 from cDNA derived from HTLV-I–transformed cells (MT-4, MT-2, and C8166) and ATL-derived IL-2–independent cell lines (MT-1, ATL-T, ED-40515(−), and ATL-25). The non–HTLV-I Jurkat T cell line was used as a control. Real-time PCR was performed in duplicate, and samples were normalized to RNU6b (U6) expression. Fold change was calculated by comparing values with Jurkat normalized miRNA expression. (B, E) Real-time PCR was performed on STAT1 from cDNA derived from HTLV-I cell lines and ATL cell lines. Real-time PCR was performed in duplicate, and samples were normalized to GAPDH expression. Fold change was calculated by comparing values with Jurkat-normalized STAT1 expression. *P* values were $<.05$. (C, F) Western blot analysis of STAT1 expression was performed from total cellular extracts of Jurkat, HTLV-I, and ATL cell lines. Extracts were normalized to actin expression. Semiquantitative analysis of Western blot data shows 165%, 158%, and 131% increase in STAT1 expression in MT-4, MT-2, and C8166, respectively, and 178%, 195%, 166%, and 148% activation of STAT1 in MT-1, ATL-T, ED-40515(−), and ATL-25, respectively, compared to Jurkat. Western blot quantification was performed by using the Java-based image processing program ImageJ. (G) Real-time PCR was performed on mature miR-150 and miR-223 from cDNA derived from ATL-derived, IL-2–dependent cell lines (LMY1, 55-T, 43T). The non–HTLV-I Jurkat T cell line was used as a control. Real-time PCR was performed in duplicate, and samples were normalized to RNU6b (U6) expression. (H) Real-time PCR was performed on STAT1 from cDNA derived from ATL-derived, IL-2–dependent cell lines (LMY1, 55-T, 43T). Real-time PCR was performed in duplicate, and data were normalized to GAPDH expression. (I) Western blot analysis of STAT1 expression was performed from total cellular extracts of Jurkat and ATL–IL-2–dependent cell lines. Extracts were normalized to actin expression. Semiquantitative analysis of Western blot data shows 225%, 188%, and 162% increase in STAT1 expression in LMY1, ATL-55T, and ATL-43T, respectively, compared to Jurkat. Western blot quantification was performed by using the Java-based image processing program ImageJ. (J) Real-time PCR was performed on mature miR-150 from ATL-derived, IL-2–dependent cell lines (LMY1, 55-T, 43T) cultured with and without IL-2 for 48 hours. Fold change was calculated by comparing values with LMY1, 55-T, and 43T cell lines cultured with IL-2. (J) Real-time PCR was performed on mature miR-150 from ATL-derived, IL-2–independent cell lines (MT-1, ATL-T) cultured with and without IL-2 for 48 hours. Fold change was calculated by comparing values with MT-1, ATL-T cell lines cultured without IL-2. (K) Western blot analysis of STAT1 expression was performed from total cellular extracts of MT-1, ATL-T cell lines cultured with and without IL-2 for 48 hours. Extracts were normalized to actin expression. Semiquantitative analysis of Western blot data shows 50.8% and 67.7% inhibition of STAT1 expression in MT-1 and ATL-T cell lines, respectively, cultured with IL-2.

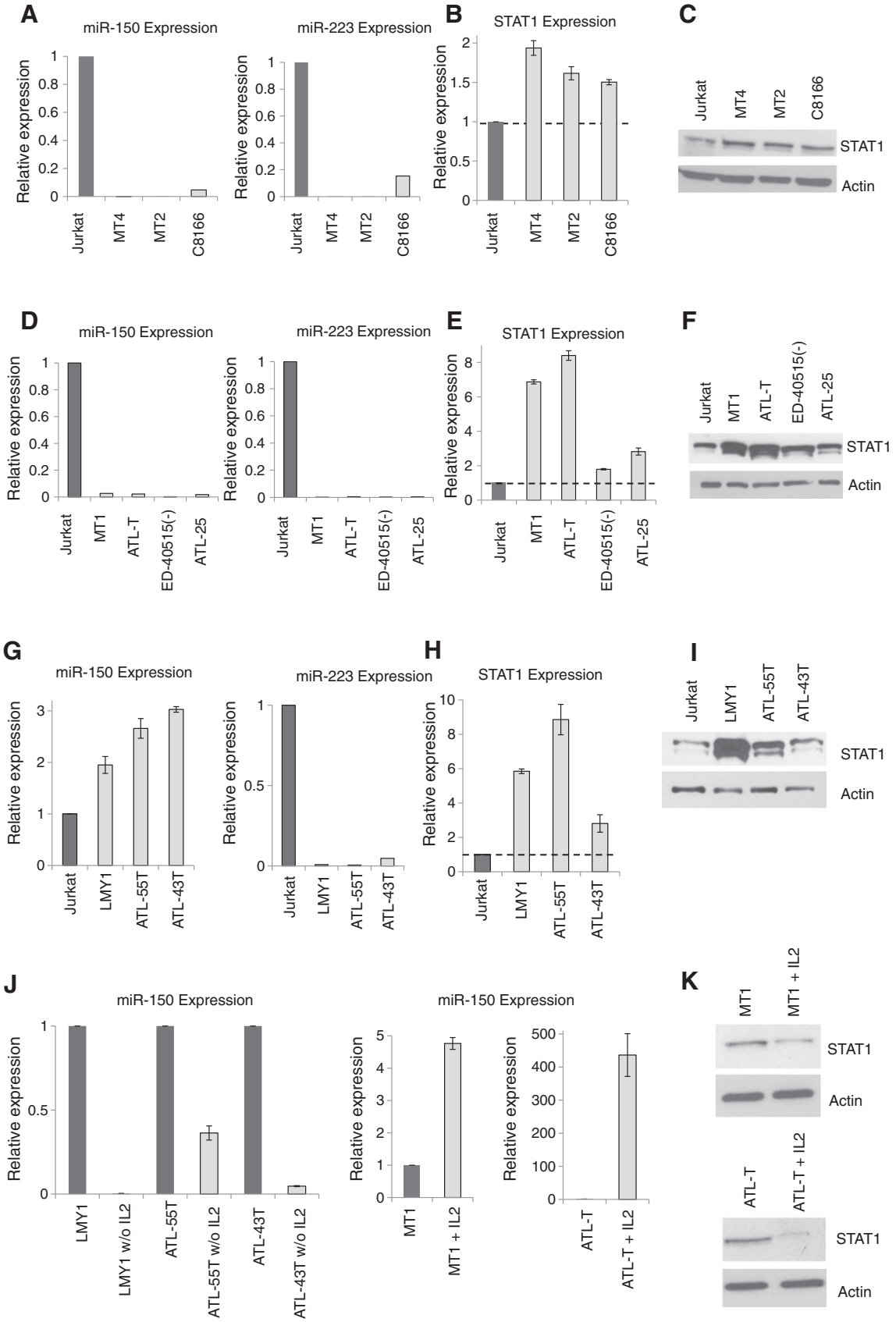
A
miR-150 Expression
Relative expression
Jurkat
MT4
MT2
C8166
miR-223 Expression
B
STAT1 Expression
C
STAT1
Actin
D
miR-150 Expression
MT1
ATL-T
ED-40515(-)
ATL-25
miR-223 Expression
E
STAT1 Expression
F
G
miR-150 Expression
LMY1
ATL-55T
ATL-43T
miR-223 Expression
H
STAT1 Expression
I
J
miR-150 Expression
LMY1 w/o IL2
ATL-55T w/o IL2
ATL-43T w/o IL2
MT1 + IL2
ATL-T + IL2
K
MT1
MT1 + IL2
ATL-T
ATL-T + IL2

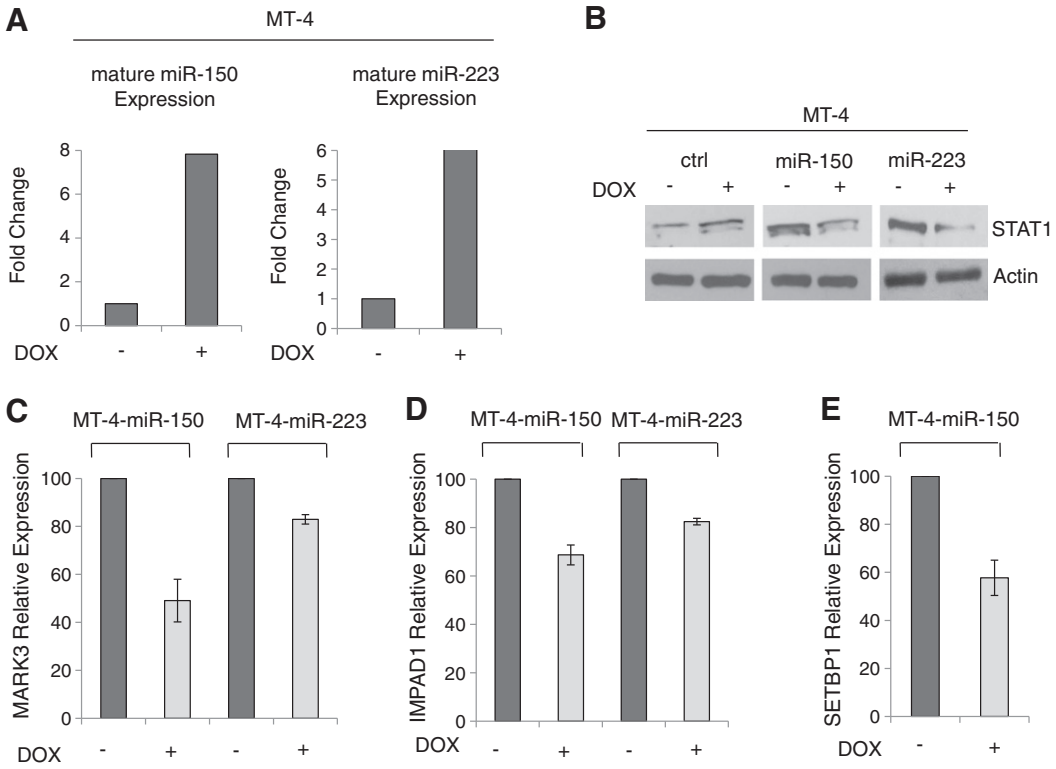


**Figure 5.** miR-150 and miR-223 inhibit STAT1 in an HTLV-I line. (A) MT-4 miR-150 and MT-4 miR-223 stable cell lines were induced with doxycycline (2 $\mu$g/ml) for 72 or 96 hours. Real-time PCR was performed on mature miR-150 and miR-223 to verify miRNA induction. Real-time PCR was performed in duplicate, and samples were normalized to U6 expression. (B) Western blot analysis of STAT1 expression from total cellular extracts of stable cell lines MT-4 miR-150 and MT-4 miR-223 treated with and without doxycycline. MT-4 pTRIPZ cells treated with and without doxycycline were used as a control. Extracts were normalized to actin expression. Semiquantitative analysis of Western blot data shows 73.1% and 71.5% inhibition of STAT1 expression in stable cell lines MT-4 miR-150 and MT-4 miR-223, respectively, treated with doxycycline compared to cells treated without doxycycline. Western blot quantification was performed by using the Java-based image processing program ImageJ. (C–E) Real-time PCR was performed on STAT1 target genes *SETBP1*, *MARK3*, and *IMPAD1* from cDNA derived from MT-4 miR-150 and MT-4 miR-223. Real-time PCR was performed in duplicate, and samples were normalized to GAPDH expression.

miR-150 (Figure 4*J*). To validate the results, we cultured ATL–IL-2–independent cell lines (MT-1, ATL-T) in the presence of IL-2 and analyzed the expression of miR-150 after 48 hours. Our results show that IL-2 signaling is associated with a significant increase in miR-150 (Figure 4*J*). Next, we analyzed STAT1 expression. The absence of IL-2 signaling in ATL–IL-2–dependent cells is not correlated with an increase in STAT1 expression (data not shown). Interestingly, IL-2 stimulation in MT-1 and ATL-T cells resulted in STAT1 down-regulation (Figure 4*K*). These results may be significant because several studies have reported that *in vivo* ATL tumor cells can produce IL-2 or IL-15 and express the high affinity IL-2 receptor α chain, CD25. We think that these observations may, in part, explain the higher levels of miR-150 found in freshly isolated uncultured ATL cells compared to *in vitro* cell lines. Despite higher expression of miR-150 in IL-2–dependent cell lines, STAT1 RNA and protein were expressed at higher levels compared to Jurkat cells (Figure 4, *H* and *I*).

### *Enforced Expression of miR-150 and miR-223 in Human T Cells Decreases STAT1 Expression and STAT1-Dependent Transcription*

To further demonstrate the effect of miR-150 and miR-223 expression on STAT1, we constructed miR-150 and miR-223 Tet-inducible expression vectors. These vectors were used to generate stable cell lines expressing pTRIPZ (control line), pTRIPZ-miR-150, or pTRIPZ-miR-223 in HTLV-I–transformed MT-4 cells. Treatment with doxycycline for 3 days efficiently restored expression of miR-150 or miR-223 in MT-4 cells (Figure 5*A*). In Jurkat T cells, induction of miR-223 was more limited. We believe that this is the result of saturation because Jurkat cells naturally express high levels of endogenous miR-223 (Figure 6*A*). Induction of miR-150 and miR-223 expression was associated with down-regulation of endogenous STAT1 expression (Figures 5*B* and 6*B*). Notably, we also confirmed that expression of several STAT1-dependent genes, MAP/microtubule affinity-regulating kinase 3 (*MARK3*), inositol monophosphatase domain containing 1 (*IMPAD1*), and SET binding protein 1 (*SETBP1*) [61], in the absence of IFN stimulation, was suppressed after induction of miR-150 and miR-223 (Figures 5, *C–E*, and 6, *C–E*). Similar results were obtained in both MT-4 and Jurkat cells. The effects were generally more pronounced in Jurkat and we believe that this may reflect the fact that these genes are also transcriptionally regulated by nuclear factor of kappa light polypeptide gene enhancer in B-cells, which is constitutively activated in MT-4 cells. SETBP1 was not studied after miR-223 overexpression because the 3′UTR for SETBP1 contains a putative miR-223 target site (data not shown). Overall, these results demonstrate that under physiological conditions miR-150 and miR-223 can reduce STAT1 expression and STAT1-dependent signaling in human leukemic T cell lines.

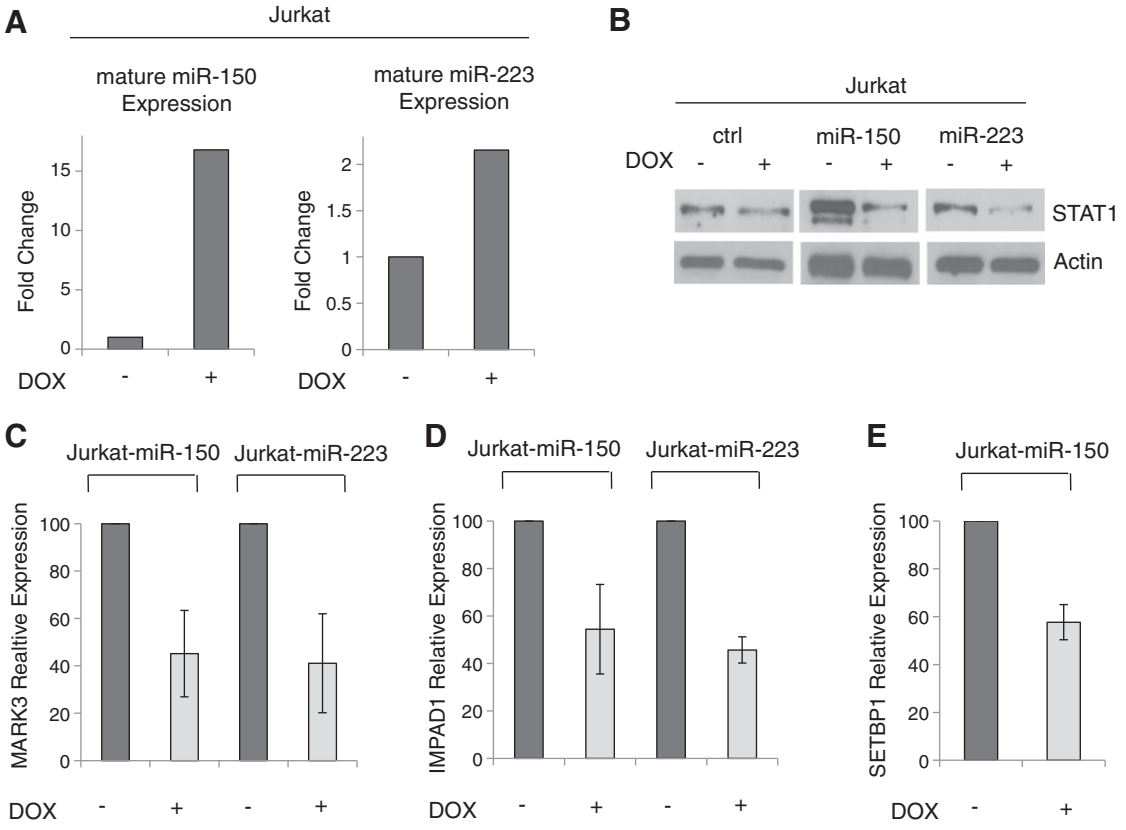


**Figure 6.** miR-150 and miR-223 inhibit STAT1 in the non–HTLV-I cell line, Jurkat. (A) Jurkat miR-150 and Jurkat miR-223 stable cell lines were induced by doxycycline (2 $\mu$g/ml) for 72 hours. Real-time PCR was performed on mature miR-150 and miR-223 to verify miRNA induction. Real-time PCR was performed in duplicate, and samples were normalized to U6 expression. (B) Western blot analysis of STAT1 expression from total cellular extracts of Jurkat miR-150 and Jurkat miR-223 stable cell lines treated with and without doxycycline. Jurkat cell lines treated with and without doxycycline were used as a control. Extracts were normalized to actin expression. Semiquantitative analysis of Western blot data shows 78.1% and 79.4% inhibition of STAT1 expression in stable cell lines Jurkat miR-150 and Jurkat miR-223, respectively, treated with doxycycline compared to cells treated without doxycycline. Western blot quantification was performed by using the Java-based image processing program ImageJ. (C–E) Real-time PCR was performed on STAT1 target genes *SETBP1*, *MARK3*, and *IMPAD1* from Jurkat miR-150 and Jurkat miR-223 cDNA treated with and without doxycycline. Real-time PCR was performed in duplicate, and samples were normalized to GAPDH expression.

### *STAT1 Is Required for the Proliferation of HTLV-I–Transformed and ATL Cells*

STAT1 expression has been frequently associated with the increased expression of genes with anti-proliferative properties, such as p21WAF or p27KIP [62]. We find no correlation between STAT1, p21WAF, or p27KIP expression in HTLV-I and ATL cell lines (Figure 9*E*). However, some reports also suggest that increased expression of STAT1 can contribute to rather than inhibit transformation and proliferation of breast cancer, head and neck cancer, melanoma, lymphoma, and leukemia cells [63]. Hence, the role of STAT1 in different cancer types may depend on other genetic alterations and other signaling pathways activated or not in these cells. To evaluate the biologic significance of STAT1 in HTLV-I–transformed cells, we first used MT-4 and MT-4 miR-150 and miR-223 inducible cell lines. Induction of either miR-150 or miR-223 expression was associated with reduced cell proliferation as determined by cell count and 2,3-bis-(2-methoxy-4-nitro- 5-sulfophenyl)-2H-tetrazolium- 5-carboxanilide (XTT) assays (Figure 7, *A* and *B*). In T-ALL, STAT1 has been shown to activate Bcl2 and promote proliferation and survival of transformed cells [64]. Consistent with these reports, we found that STAT1 was involved in Bcl2 expression in MT-4 and Jurkat inducible cell lines (Figure 7*D*). Treatment with doxycycline for 3 days significantly increased Bcl2 expression compared to untreated cells (Figure 7*C*). For this reason, we analyzed Bcl2 expression in treated MT-4 miR-150, MT-4 miR-223, Jurkat-miR-150, and Jurkat-miR-223 cells compared to the treated MT-4 and Jurkat control. As expected, the induction significantly decreased Bcl2 expression in MT-4 and Jurkat cell lines (Figure 7*D*). To verify the specificity of these results, we included Western blot analysis of untreated MT-4 and Jurkat inducible cell lines. The results show no change or an increased level of Bcl2 expression compared to the control (Figure 7*D*). Because many T-ALL leukemic cells are dependent on the TYK2-STAT1-BCL2 pathway for continued survival, we analyzed the sequence of Tyk2 in several ATL samples. However, no mutation was found in the kinase domain of Tyk2 in ATL samples, but a high frequency of Tyk2 V362F single nucleotide polymorphism was found. The possible significance of this mutation remains to be established.

We are aware that miR-150 and miR-223 likely exert some of their effect through STAT1-independent pathways. To demonstrate a direct function of STAT1 in HTLV-I–transformed cells, we next generated a lentiviral vector expressing shRNA to knock down STAT1 expression. Functionality was first verified following infection

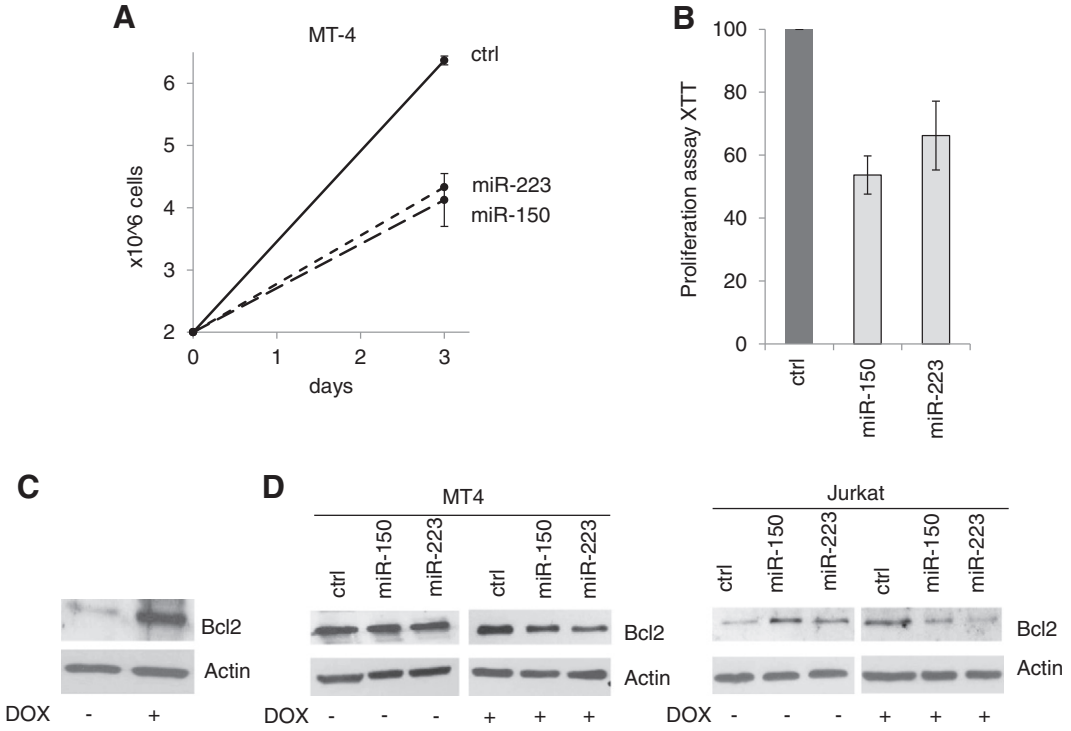


**Figure 7.** Exogenous expression of miR-150 and miR-223 inhibits proliferation of HTLV-I cells. (A, B) MT-4 pTRIPZ, miR-150, and miR-223 inducible cell lines were induced with doxycycline (2 $\mu$g/ml). After 72 hours, cell count and XTT assays were performed; *P* value was <.05. MT-4 pTRIPZ cells induced with doxycycline were used as a control. (C) Western blot analysis of Bcl2 expression from total cellular extracts of Jurkat cell lines treated with and without doxycycline. Semiquantitative analysis of Western blot data shows a 229% increase in Bcl2 expression. Western blot quantification was performed by using the Java-based image processing program ImageJ. (D) Western blot analysis of Bcl2 expression from total cellular extracts of MT-4 and Jurkat inducible cell lines treated with and without doxycycline. Extracts were normalized to actin expression. Semiquantitative analysis of Western blot data shows 45.8% and 67.7% inhibition of Bcl2 expression in stable cell lines MT-4 miR-150 and MT-4 miR-223, respectively, treated with doxycycline compared to MT-4 pTRIPZ cell lines and 50% and 62% inhibition in Jurkat miR-150 and Jurkat miR-223, respectively, compared to Jurkat. Western blot quantification was performed by using the Java-based image processing program ImageJ.

of 293T cells (Figure 8, *A* and *B*). shRNA STAT1 efficiently reduced STAT1 and Bcl2 expression (Figure 8*B*). We confirmed a reduction in STAT1 expression in the HTLV-I–transformed MT-2 transduced cells by more than 50% (Figure 8*C*), which was associated with a disruption in cell cycle progression, a 24.3% reduction in the number of cells in S phase and an accumulation of cells in $G_2$/M (Figure 8*D*). To confirm that these observations were not specific to MT-2 and could be generalized to other HTLV-I–transformed cells, we transduced MT-2, C91PL, and MT-4 HTLV-I–transformed cells and an MT-1 ATL cell line. Transduction of STAT1 shRNA was first confirmed by using RT-PCR (Figure 9*A*). STAT1 down-regulation was associated with reduced cell proliferation as determined by cell count, XTT assays, and bromodeoxyuridine incorporation (Figure 9, *B–D*). Together our results demonstrate that STAT1 is required for the proliferation of HTLV-I–transformed and ATL cells.

### *Increased STAT1 and MHC-I Expression in ATL Cells*

Since our results demonstrate an important role of STAT1 in proliferation of HTLV-I–transformed cells, we then wanted to investigate expression of STAT1 in freshly isolated uncultured ATL samples. We next analyzed RNA samples from 35 patients with acute ATL and 9 HDs by RT-PCR. Our results showed that STAT1 was significantly elevated in patients with ATL compared with HD (almost three-fold higher; Figure 10*A*). Early studies suggest that ATL cells originate within the helper-inducer T cell subtype and have a common cytokine production profile including IL-1α, IL-1β, tumour necrosis factor alpha, IFN-γ, and granulocyte-macrophage colony-stimulating-factor [65]. Among these factors, IFN-γ is a well-known potent inducer of MHC class I through activation of the JAK/STAT1/interferon regulatory factor 1 signal transduction pathway [66]. Tumor cells with low or no MHC-I cell surface expression may escape recognition by anti-tumor T cells but are highly sensitive to NK-mediated killing. In fact, increased expression of MHC-I is one important mechanism that allows for immune escape [67–70]. We then investigated the expression of MHC-I in ATL and HD samples. Overall, ATL samples have significantly higher expression of MHC-I when compared to HD samples (Figure 10*B*).

## Discussion

In this study, we demonstrate for the first time that miR-150 and miR-223 target the STAT1 3′UTR, reduce STAT1 expression, and reduce both IFN-dependent and IFN-independent STAT1-mediated signaling. We have previously reported that miR-150 and miR-223 are differentially regulated in HTLV-I cells transformed *in vitro* and *in vivo* ATL samples, suggesting that ATL cells and *in vitro* established HTLV-I cell lines may derive from distinct cellular populations. In this study, we have shown that IL-2R–mediated signaling can increase miR-150 expression in ATL cells. Previous

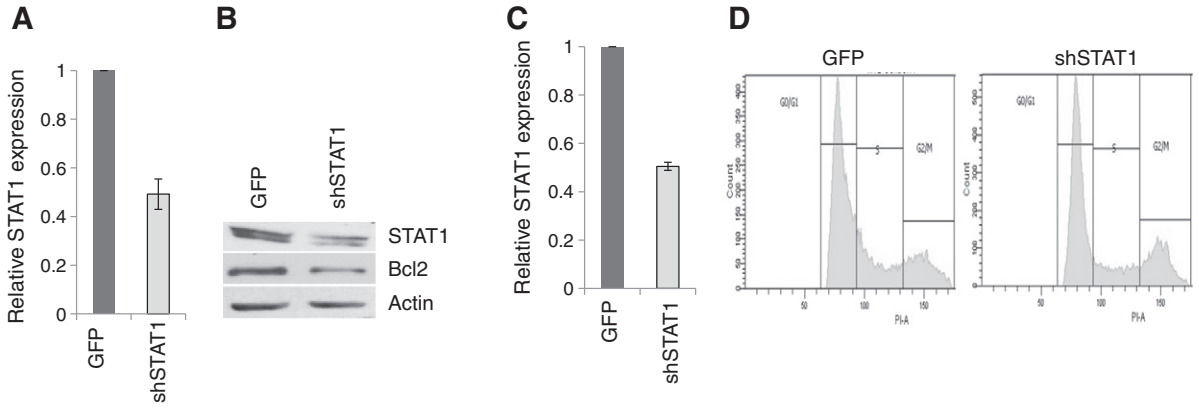


**Figure 8.** Inhibition of STAT1 expression in the HTLV-I cell, MT-2, results in cell cycle disruption. (A) Real-time PCR analysis of STAT1 expression was performed from total cDNA from 293T cells infected with pSIH1-GFP and pSIH1-GFP-shSTAT1. Extracts were analyzed 48 hours after transfection and normalized to GAPDH expression. *P* value was < .05. (B) Western blot analysis of Bcl2 and STAT1 expression from total cellular extracts of 293T cells infected with lentiviruses expressing shSTAT1 or empty lentivirus (pSIH1-GFP) used as a control. Extracts were normalized to actin expression. Semiquantitative analysis of Western blot data shows 70.9% of Bcl2 expression and 70.4% inhibition of STAT1 expression in 293T cells infected with shSTAT1, compared to the control. Western blot quantification was performed by using the Java-based image processing program ImageJ. (C) Real-time PCR analysis of STAT1 expression was performed from total cDNA from MT-2 cells transfected with pSIH1-GFP or pSIH1-GFP-shSTAT1. Extracts were analyzed 48 hours after transfection and normalized to GAPDH expression. *P* value was < .05. (D) Cell-cycle analysis of MT-2 cells infected with lentiviruses encoding vector control (pSIH1-GFP) and shSTAT1. Cell-cycle analysis demonstrated a 24.3% reduction in the number of cells in S phase compared to GFP control.

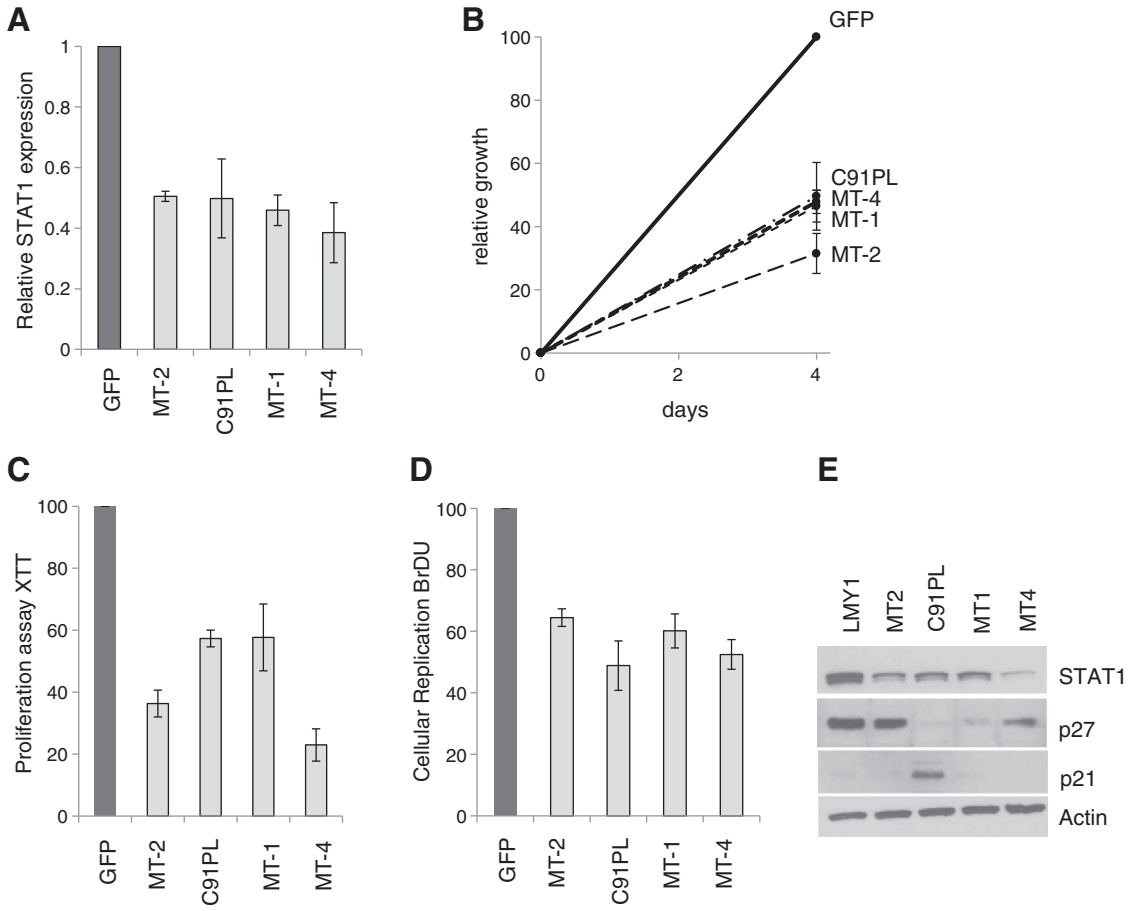


**Figure 9.** Inhibition of STAT1 expression results in a decrease in cellular proliferation in HTLV-I cells. (A) Real-time PCR analysis of STAT1 expression was performed from total cDNA from MT-2, C91PL, MT-1, and MT-4 cells infected with pSIH1-GFP or pSIH1-GFP-shSTAT1. Extracts were analyzed 48 hours after infection and normalized to GAPDH expression. *P* values were < .05. (B) MT-2, C91PL, MT-1, and MT-4 cells were infected with lentivirus encoding vector control (pSIH1-GFP) or shSTAT1. After 48 hours, cells were counted for proliferation (B) and XTT proliferation (C) assays, and bromodeoxyuridine assays were performed (D). *P* values were < .05 (B–D). (E) Western blot analysis of p21, p27, and STAT1expression from total cellular extracts of LMY1, MT-2, C91PL, MT-1, and MT-4. Extracts were normalized to actin expression.

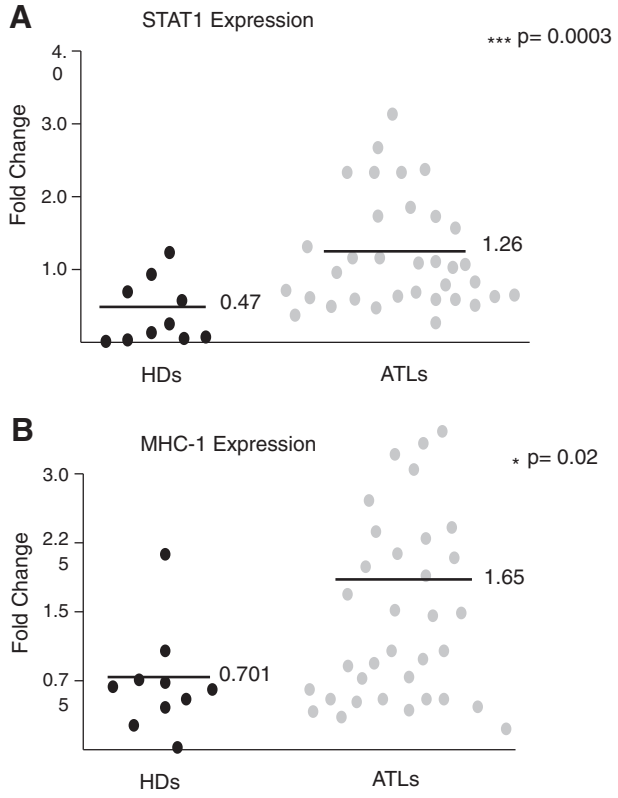


**Figure 10.** STAT1 expression correlates with increased MHC-I expression in ATL patient samples. (A) Real-time PCR analysis of STAT1 expression from cDNA derived from PBMCs of patients with ATL. Samples were normalized to GAPDH expression, and the fold change was calculated by comparing values to HD's normalized gene expression. (B) Real-time PCR analysis of MHC-I expression from cDNA derived from PBMCs of patients with ATL. Samples were normalized to GAPDH expression, and the fold change was calculated by comparing values to HD's normalized gene expression. Statistical analysis was performed by using unpaired two-sided Student's *t* test.

studies have demonstrated that ATL cells overexpress an IL-2Rα chain (CD25). Additional studies have shown that ATL cells may produce or respond to IL-2 or other IL-2Rγ chain user cytokines in the microenvironment [71–75]. In contrast, *in vitro* transformed cells do express CD25 but do not produce IL-2. With regard to miR-223, it has been previously shown that E2F1 represses the miR-223 promoter [26,76]. Interestingly, viral HTLV-I bZIP factor mRNA increases the expression and transcriptional activity of E2F1 [77]. In contrast to other viral genes, HTLV-I bZIP factor expression is consistently increased in ATL cells *in vivo* [77]. These observations can, in part, explain the differential regulation of miR-223 expression between *in vitro* and *in vivo* HTLV-I–transformed cells. Others have shown that overexpression of miR-150 in bone marrow progenitor cells resulted in modest inhibition of cell proliferation [3], suggesting low side effects. Therefore, reinstating miR-150 expression may provide an effective therapeutic strategy to treat HTLV-I leukemia. Our studies also revealed that STAT1 expression is inversely correlated to that of miR-150 and miR-223 in HTLV-I–transformed and ATL cells and is generally increased in HTLV-I–transformed cells. Several studies have shown that an increase in STAT1 expression is associated with radio-protection of cancer cells. Since HTLV-I–transformed cells are notoriously resistant to high dose radiotherapy, it is possible that increased STAT1 expression plays a role in the resistance to high dose radiotherapy and warrants additional studies. STAT1 has been associated with both tumor suppressor and tumor promoting activities [78,79]. Our studies suggest that in HTLV-I–infected cells STAT1 has a tumor promoting effect since inhibition of STAT1 expression and STAT1-dependent transcription through miR-150 or miR-223 or directly by shRNA targeting resulted in reduced proliferation of HTLV-I–transformed and ATL cells. In addition, STAT1 may play an important role in the immune-suppressive status observed in patients with ATL and allow HTLV-I–transformed cells to evade NK-mediated killing. Along these lines, knockout mice studies showed that the IFN-α receptor 1 and STAT1 are both required for normal tumor Treg frequencies and the release of IL-10, a potent inhibitor of NK activity, in the tumor microenvironment. Indeed, high levels of IL-10 in the serum of patients with acute ATL have been reported. Furthermore, increased STAT1 as observed in patients with ATL may be involved in higher levels of MHC-I expression. Although MHC-I is not a direct target for STAT1, previous studies have demonstrated that STAT1 plays an essential role in chromatin decondensation of the MHC locus through interactions with the remodeling brahma protein-like 1 factor [80]. As indicated above, increased expression of MHC-I on tumor cells has been associated with escape from NK-mediated killing of tumor cells and more aggressive tumor phenotypes [81,82]. Our results showed that patients with ATL with a higher expression of STAT1 displayed higher levels of MHC-I as well. Since STAT1 plays an important role in regulation of inducible nitric oxide synthase activity, it is possible that it participates in upregulated expression of inducible nitric oxide synthase in ATL cells.

There are also some unforeseen observations in our study. First, suppressor of cytokine signaling 1, a terminator of STAT1-dependent signaling, has been reported to be activated in HTLV-I–transformed cells through a mechanism involving the Tax oncoprotein [83]. However, it should be remembered here that *in vivo* about half of ATL samples have no detectable Tax expression [84], and therefore, the ability of suppressor of cytokine signaling 1 to block STAT1 may vary greatly among patients and is currently under investigation. In addition, several kinases, including cyclin-dependent kinase 8, can phosphorylate STAT1 at serine 727 to restrain NK cell cytotoxicity by reducing expression of perforin and granzyme B [85]. Targeted inhibition of cyclin-dependent kinase 8-mediated STAT1 phosphorylation at serine 727 may represent a possible approach to stimulate NK cell–mediated tumor surveillance in patients with ATL.

Despite expression of both miR-150 and miR-223 in freshly isolated ATL samples, STAT1 did not seem to be affected, as both STAT1 RNA and protein were increased in a majority of ATL samples. These data suggest that in ATL patient cells miR-150 and miR-223 may not be able to efficiently target the STAT1 3′UTR. Although the reason for this deficiency is unclear, it is possible that other higher affinity gene targets expressed at higher levels act as competitors and sequester miR-150 and miR-223 or that the sequence or the spatial structure/folding of the STAT1 3′UTR is altered in ATL cells *in vivo* and warrants additional future studies.

Targeted inhibition of STAT1 has been investigated in various types of leukemia. For instance, treatment of acute myeloid cells (AML) with retinoic acid resulted in an increased STAT1 expression and reduced proliferation [80]. In addition, STAT1 has been shown to play a key role in dasatinib-induced differentiation of acute myeloid cells (AML) and in Bryostatin-1–induced differentiation of CLL cells [61,86]. The results presented here suggest that STAT1

may represent a target for therapeutic intervention in some patients with ATL.

## Acknowledgement

The authors thank Brandi Miller for editorial assistance.

## References

[1] Papakonstantinou N, Ntoufa S, Chartomatsidou E, Papadopoulos G, Hatzigeorgiou A, Anagnostopoulos A, Chlichlia K, Ghia P, Muzio M, and Belessi C, et al (2013). Differential microRNA profiles and their functional implications in different immunogenetic subsets of chronic lymphocytic leukemia. *Mol Med* **19**, 115–123.

[2] Mraz M, Chen L, Rassenti LZ, Ghia EM, Li H, Jepsen K, Smith EN, Messer K, Frazer KA, and Kipps TJ (2014). miR-150 influences B-cell receptor signaling in chronic lymphocytic leukemia by regulating expression of GAB1 and FOXP1. *Blood* **124**, 84–95.

[3] Morris VA, Zhang A, Yang T, Stirewalt DL, Ramamurthy R, Meshinchi S, and Oehler VG (2013). MicroRNA-150 expression induces myeloid differentiation of human acute leukemia cells and normal hematopoietic progenitors. *PLoS One* **8**, e75815.

[4] Machova PK, Lopotova T, Klamova H, Burda P, Trneny M, Stopka T, and Moravcova J (2011). Expression patterns of microRNAs associated with CML phases and their disease related targets. *Mol Cancer* **10**, 41.

[5] Xu L, Liang YN, Luo XQ, Liu XD, and Guo HX (2011). Association of miRNAs expression profiles with prognosis and relapse in childhood acute lymphoblastic leukemia. *Zhonghua Xue Ye Xue Za Zhi* **32**, 178–181.

[6] Zhao JJ, Lin J, Lwin T, Yang H, Guo J, Kong W, Dessureault S, Moscinski LC, Rezania D, and Dalton WS, et al (2010). microRNA expression profile and identification of miR-29 as a prognostic marker and pathogenetic factor by targeting CDK6 in mantle cell lymphoma. *Blood* **115**, 2630–2639.

[7] Cao M, Hou D, Liang H, Gong F, Wang Y, Yan X, Jiang X, Wang C, Zhang J, and Zen K, et al (2014). miR-150 promotes the proliferation and migration of lung cancer cells by targeting SRC kinase signalling inhibitor 1. *Eur J Cancer* **50**, 1013–1024.

[8] Avery-Kiejda KA, Braye SG, Mathe A, Forbes JF, and Scott RJ (2014). Decreased expression of key tumour suppressor microRNAs is associated with lymph node metastases in triple negative breast cancer. *BMC Cancer* **14**, 51.

[9] Huang S, Chen Y, Wu W, Ouyang N, Chen J, Li H, Liu X, Su F, Lin L, and Yao Y (2013). miR-150 promotes human breast cancer growth and malignant behavior by targeting the pro-apoptotic purinergic P2X7 receptor. *PLoS One* **8**, e80707.

[10] Xiao C, Calado DP, Galler G, Thai TH, Patterson HC, Wang J, Rajewsky N, Bender TP, and Rajewsky K (2007). MiR-150 controls B cell differentiation by targeting the transcription factor c-Myb. *Cell* **131**, 146–159.

[11] Ghisi M, Corradin A, Basso K, Frasson C, Serafin V, Mukherjee S, Mussolin L, Ruggero K, Bonanno L, and Guffanti A, et al (2011). Modulation of microRNA expression in human T-cell development: targeting of NOTCH3 by miR-150. *Blood* **117**, 7053–7062.

[12] Bousquet M, Zhuang G, Meng C, Ying W, Cheruku PS, Shie AT, Wang S, Ge G, Wong P, and Wang G, et al (2013). miR-150 blocks MLL-AF9-associated leukemia through oncogene repression. *Mol Cancer Res* **11**, 912–922.

[13] Wu Q, Jin H, Yang Z, Luo G, Lu Y, Li K, Ren G, Su T, Pan Y, and Feng B, et al (2010). MiR-150 promotes gastric cancer proliferation by negatively regulating the pro-apoptotic gene EGR2. *Biochem Biophys Res Commun* **392**, 340–345.

[14] Watanabe A, Tagawa H, Yamashita J, Teshima K, Nara M, Iwamoto K, Kume M, Kameoka Y, Takahashi N, and Nakagawa T, et al (2011). The role of microRNA-150 as a tumor suppressor in malignant lymphoma. *Leukemia* **25**, 1324–1334.

[15] Wong QW, Lung RW, Law PT, Lai PB, Chan KY, To KF, and Wong N (2008). MicroRNA-223 is commonly repressed in hepatocellular carcinoma and potentiates expression of Stathmin1. *Gastroenterology* **135**, 257–269.

[16] Stamatopoulos B, Meuleman N, Haibe-Kains B, Saussoy P, Van Den Neste E, Michaux L, Heimann P, Martiat P, Bron D, and Lagneaux L (2009). microRNA-29c and microRNA-223 down-regulation has in vivo significance in chronic lymphocytic leukemia and improves disease risk stratification. *Blood* **113**, 5237–5245.

[17] Mi S, Lu J, Sun M, Li Z, Zhang H, Neilly MB, Wang Y, Qian Z, Jin J, and Zhang Y, et al (2007). MicroRNA expression signatures accurately discriminate acute lymphoblastic leukemia from acute myeloid leukemia. *Proc Natl Acad Sci U S A* **104**, 19971–19976.

[18] Liu TY, Chen SU, Kuo SH, Cheng AL, and Lin CW (2010). E2A-positive gastric MALT lymphoma has weaker plasmacytoid infiltrates and stronger expression of the memory B-cell-associated miR-223: possible correlation with stage and treatment response. *Mod Pathol* **23**, 1507–1517.

[19] Laios A, O'Toole S, Flavin R, Martin C, Kelly L, Ring M, Finn SP, Barrett C, Loda M, and Gleeson N, et al (2008). Potential role of miR-9 and miR-223 in recurrent ovarian cancer. *Mol Cancer* **7**, 35.

[20] Kumar V, Palermo R, Talora C, Campese AF, Checquolo S, Bellavia D, Tottone L, Testa G, Miele E, and Indraccolo S, et al (2014). Notch and NF-kB signaling pathways regulate miR-223/FBXW7 axis in T-cell acute lymphoblastic leukemia. *Leukemia* **28**, 2324–2335.

[21] Lee JE, Hong EJ, Nam HY, Kim JW, Han BG, and Jeon JP (2011). MicroRNA signatures associated with immortalization of EBV-transformed lymphoblastoid cell lines and their clinical traits. *Cell Prolif* **44**, 59–66.

[22] Li J, Guo Y, Liang X, Sun M, Wang G, De W, and Wu W (2012). MicroRNA-223 functions as an oncogene in human gastric cancer by targeting FBXW7/hCdc4. *J Cancer Res Clin Oncol* **138**, 763–774.

[23] Li X, Zhang Y, Zhang H, Liu X, Gong T, Li M, Sun L, Ji G, Shi Y, and Han Z, et al (2011). miRNA-223 promotes gastric cancer invasion and metastasis by targeting tumor suppressor EPB41L3. *Mol Cancer Res* **9**, 824–833.

[24] Sun G, Li H, and Rossi JJ (2010). Sequence context outside the target region influences the effectiveness of miR-223 target sites in the RhoB 3'UTR. *Nucleic Acids Res* **38**, 239–252.

[25] Wong QW, Lung RW, Law PT, Lai PB, Chan KY, To KF, and Wong N (2008). MicroRNA-223 is commonly repressed in hepatocellular carcinoma and potentiates expression of Stathmin1. *Gastroenterology* **135**, 257–269.

[26] Pulikkan JA, Dengler V, Peramangalam PS, Peer Zada AA, Muller-Tidow C, Bohlander SK, Tenen DG, and Behre G (2010). Cell-cycle regulator E2F1 and microRNA-223 comprise an autoregulatory negative feedback loop in acute myeloid leukemia. *Blood* **115**, 1768–1778.

[27] Haneklaus M, Gerlic M, O'Neill LA, and Masters SL (2013). miR-223: infection, inflammation and cancer. *J Intern Med* **274**, 215–226.

[28] Gallo RC (2005). History of the discoveries of the first human retroviruses: HTLV-1 and HTLV-2. *Oncogene* **24**, 5926–5930.

[29] Poiesz BJ, Ruscetti FW, Gazdar AF, Bunn PA, Minna JD, and Gallo RC (1980). Detection and isolation of type C retrovirus particles from fresh and cultured lymphocytes of a patient with cutaneous T-cell lymphoma. *Proc Natl Acad Sci U S A* **77**, 7415–7419.

[30] Gessain A, Barin F, Vernant JC, Gout O, Maurs L, Calender A, and de TG (1985). Antibodies to human T-lymphotropic virus type-I in patients with tropical spastic paraparesis. *Lancet* **2**, 407–410.

[31] Osame M, Matsumoto M, Usuku K, Izumo S, Ijichi N, Amitani H, Tara M, and Igata A (1987). Chronic progressive myelopathy associated with elevated antibodies to human T-lymphotropic virus type I and adult T-cell leukemialike cells. *Ann Neurol* **21**, 117–122.

[32] Sampey GC, Van DR, Currer R, Das R, Narayanan A, and Kashanchi F (2012). Complex role of microRNAs in HTLV-1 infections. *Front Genet* **3**, 295.

[33] D'Agostino DM, Zanovello P, Watanabe T, and Ciminale V (2012). The microRNA regulatory network in normal- and HTLV-1-transformed T cells. *Adv Cancer Res* **113**, 45–83.

[34] Yamagishi M, Nakano K, Miyake A, Yamochi T, Kagami Y, Tsutsumi A, Matsuda Y, Sato-Otsubo A, Muto S, and Utsunomiya A, et al (2012). Polycomb-mediated loss of miR-31 activates NIK-dependent NF-kappaB pathway in adult T cell leukemia and other cancers. *Cancer Cell* **21**, 121–135.

[35] Tomita M, Tanaka Y, and Mori N (2012). MicroRNA miR-146a is induced by HTLV-1 tax and increases the growth of HTLV-1-infected T-cells. *Int J Cancer* **130**, 2300–2309.

[36] Bellon M, Lepelletier Y, Hermine O, and Nicot C (2009). Deregulation of microRNA involved in hematopoiesis and the immune response in HTLV-I adult T-cell leukemia. *Blood* **113**, 4914–4917.

[37] Bouzar AB and Willems L (2008). How HTLV-1 may subvert miRNAs for persistence and transformation. *Retrovirology* **5**, 101.

[38] Gessain A and Mahieux R (2012). Tropical spastic paraparesis and HTLV-1 associated myelopathy: clinical, epidemiological, virological and therapeutic aspects. *Rev Neurol (Paris)* **168**, 257–269.

[39] Watanabe T (2011). Current status of HTLV-1 infection. *Int J Hematol* **94**, 430–434.

[40] Yasunaga J and Matsuoka M (2011). Molecular mechanisms of HTLV-1 infection and pathogenesis. *Int J Hematol* **94**, 435–442.

[41] Bellon M, Baydoun HH, Yao Y, and Nicot C (2010). HTLV-I Tax-dependent and -independent events associated with immortalization of human primary T lymphocytes. *Blood* **115**, 2441–2448.

[42] Chaib-Mezrag H, Lemacon D, Fontaine H, Bellon M, Bai XT, Drac M, Coquelle A, and Nicot C (2014). Tax impairs DNA replication forks and increases DNA breaks in specific oncogenic genome regions. *Mol Cancer* **13**, 205.

[43] Baydoun HH, Bai XT, Shelton S, and Nicot C (2012). HTLV-I tax increases genetic instability by inducing DNA double strand breaks during DNA replication and switching repair to NHEJ. *PLoS One* **7**, e42226.
[44] Matsuoka M and Yasunaga J (2013). Human T-cell leukemia virus type 1: replication, proliferation and propagation by Tax and HTLV-1 bZIP factor. *Curr Opin Virol* **3**, 684–691.
[45] Currer R, Van DR, Jaworski E, Guendel I, Sampey G, Das R, Narayanan A, and Kashanchi F (2012). HTLV tax: a fascinating multifunctional co-regulator of viral and cellular pathways. *Front Microbiol* **3**, 406.
[46] Marriott SJ and Semmes OJ (2005). Impact of HTLV-I Tax on cell cycle progression and the cellular DNA damage repair response. *Oncogene* **24**, 5986–5995.
[47] Pise-Masison CA, Jeong SJ, and Brady JN (2005). Human T cell leukemia virus type 1: the role of Tax in leukemogenesis. *Arch Immunol Ther Exp (Warsz)* **53**, 283–296.
[48] Harhaj EW and Harhaj NS (2005). Mechanisms of persistent NF-kappaB activation by HTLV-I tax. IUBMB. *Life* **57**, 83–91.
[49] Takemoto S, Mulloy JC, Cereseto A, Migone TS, Patel BK, Matsuoka M, Yamaguchi K, Takatsuki K, Kamihira S, and White JD, et al (1997). Proliferation of adult T cell leukemia/lymphoma cells is associated with the constitutive activation of JAK/STAT proteins. *Proc Natl Acad Sci U S A* **94**, 13897–13902.
[50] Migone TS, Lin JX, Cereseto A, Mulloy JC, O'Shea JJ, Franchini G, and Leonard WJ (1995). Constitutively activated Jak-STAT pathway in T cells transformed with HTLV-I. *Science* **269**, 79–81.
[51] Rajasingh J, Raikwar HP, Muthian G, Johnson C, and Bright JJ (2006). Curcumin induces growth-arrest and apoptosis in association with the inhibition of constitutively active JAK-STAT pathway in T cell leukemia. *Biochem Biophys Res Commun* **340**, 359–368.
[52] Kirken RA, Erwin RA, Wang L, Wang Y, Rui H, and Farrar WL (2000). Functional uncoupling of the Janus kinase 3-Stat5 pathway in malignant growth of human T cell leukemia virus type 1-transformed human T cells. *J Immunol* **165**, 5097–5104.
[53] Ju W, Zhang M, Jiang JK, Thomas CJ, Oh U, Bryant BR, Chen J, Sato N, Tagaya Y, and Morris JC, et al (2011). CP-690,550, a therapeutic agent, inhibits cytokine-mediated Jak3 activation and proliferation of T cells from patients with ATL and HAM/TSP. *Blood* **117**, 1938–1946.
[54] Decker T, Stockinger S, Karaghiosoff M, Muller M, and Kovarik P (2002). IFNs and STATs in innate immunity to microorganisms. *J Clin Invest* **109**, 1271–1277.
[55] Kovacic B, Stoiber D, Moriggl R, Weisz E, Ott RG, Kreibich R, Levy DE, Beug H, Freissmuth M, and Sexl V (2006). STAT1 acts as a tumor promoter for leukemia development. *Cancer Cell* **10**, 77–87.
[56] Sanda T, Tyner JW, Gutierrez A, Ngo VN, Glover J, Chang BH, Yost A, Ma W, Fleischman AG, and Zhou W, et al (2013). TYK2-STAT1-BCL2 pathway dependence in T-cell acute lymphoblastic leukemia. *Cancer Discov* **3**, 564–577.
[57] Maeda M, Shimizu A, Ikuta K, Okamoto H, Kashihara M, Uchiyama T, Honjo T, and Yodoi J (1985). Origin of human T-lymphotrophic virus I-positive T cell lines in adult T cell leukemia. Analysis of T cell receptor gene rearrangement. *J Exp Med* **162**, 2169–2174.
[58] Yamada Y, Ohmoto Y, Hata T, Yamamura M, Murata K, Tsukasaki K, Kohno T, Chen Y, Kamihira S, and Tomonaga M (1996). Features of the cytokines secreted by adult T cell leukemia (ATL) cells. *Leuk Lymphoma* **21**, 443–447.
[59] Zhao T, Satou Y, Sugata K, Miyazato P, Green PL, Imamura T, and Matsuoka M (2011). HTLV-1 bZIP factor enhances TGF-beta signaling through p300 coactivator. *Blood* **118**, 1865–1876.
[60] Rauch I, Muller M, and Decker T (2013). The regulation of inflammation by interferons and their STATs. *JAKSTAT* **2**, e23820.
[61] Dimco G, Knight RA, Latchman DS, and Stephanou A (2010). STAT1 interacts directly with cyclin D1/Cdk4 and mediates cell cycle arrest. *Cell Cycle* **9**, 4638–4649.
[62] Haura EB, Turkson J, and Jove R (2005). Mechanisms of disease: Insights into the emerging role of signal transducers and activators of transcription in cancer. *Nat Clin Pract Oncol* **2**, 315–324.
[63] Sanda T, Tyner JW, Gutierrez A, Ngo VN, Glover J, Chang BH, Yost A, Ma W, Fleischman AG, and Zhou W, et al (2013). TYK2-STAT1-BCL2 pathway dependence in T-cell acute lymphoblastic leukemia. *Cancer Discov* **3**, 564–577.
[64] Yamada Y, Ohmoto Y, Hata T, Yamamura M, Murata K, Tsukasaki K, Kohno T, Chen Y, Kamihira S, and Tomonaga M (1996). Features of the cytokines secreted by adult T cell leukemia (ATL) cells. *Leuk Lymphoma* **21**, 443–447.
[65] Lee CK, Gimeno R, and Levy DE (1999). Differential regulation of constitutive major histocompatibility complex class I expression in T and B lymphocytes. *J Exp Med* **190**, 1451–1464.
[66] Cerwenka A and Lanier LL (2001). Natural killer cells, viruses and cancer. *Nat Rev Immunol* **1**, 41–49.
[67] Colucci F, Caligiuri MA, and Di Santo JP (2003). What does it take to make a natural killer? *Nat Rev Immunol* **3**, 413–425.
[68] Ljunggren HG and Karre K (1986). Experimental strategies and interpretations in the analysis of changes in MHC gene expression during tumour progression. Opposing influences of T cell and natural killer mediated resistance? *J Immunogenet* **13**, 141–151.
[69] Mocikat R, Braumuller H, Gumy A, Egeter O, Ziegler H, Reusch U, Bubeck A, Louis J, Mailhammer R, and Riethmuller G, et al (2003). Natural killer cells activated by MHC class I(low) targets prime dendritic cells to induce protective CD8 T cell responses. *Immunity* **19**, 561–569.
[70] Satoh M, Toma H, Sugahara K, Etoh K, Shiroma Y, Kiyuna S, Takara M, Matsuoka M, Yamaguchi K, and Nakada K, et al (2002). Involvement of IL-2/IL-2R system activation by parasite antigen in polyclonal expansion of CD4(+)25(+) HTLV-1-infected T-cells in human carriers of both HTLV-1 and S. stercoralis. *Oncogene* **21**, 2466–2475.
[71] Yamada Y, Sugawara K, Hata T, Tsuruta K, Moriuchi R, Maeda T, Atogami S, Murata K, Fujimoto K, and Kohno T, et al (1998). Interleukin-15 (IL-15) can replace the IL-2 signal in IL-2-dependent adult T-cell leukemia (ATL) cell lines: expression of IL-15 receptor alpha on ATL cells. *Blood* **91**, 4265–4272.
[72] Waldmann TA, White JD, Goldman CK, Top L, Grant A, Bamford R, Roessler E, Horak ID, Zaknoen S, and Kasten-Sportes C, et al (1993). The interleukin-2 receptor: a target for monoclonal antibody treatment of human T-cell lymphotrophic virus I-induced adult T-cell leukemia. *Blood* **82**, 1701–1712.
[73] Maeda M, Arima N, Daitoku Y, Kashihara M, Okamoto H, Uchiyama T, Shirono K, Matsuoka M, Hattori T, and Takatsuki K, et al (1987). Evidence for the interleukin-2 dependent expansion of leukemic cells in adult T cell leukemia. *Blood* **70**, 1407–1411.
[74] Arima N, Daitoku Y, Ohgaki S, Fukumori J, Tanaka H, Yamamoto Y, Fujimoto K, and Onoue K (1986). Autocrine growth of interleukin 2-producing leukemic cells in a patient with adult T cell leukemia. *Blood* **68**, 779–782.
[75] McGirt LY, Adams CM, Baerenwald DA, Zwerner JP, Zic JA, and Eischen CM (2014). miR-223 regulates cell growth and targets proto-oncogenes in mycosis fungoides/cutaneous T-cell lymphoma. *J Invest Dermatol* **134**, 1101–1107.
[76] Satou Y, Yasunaga J, Yoshida M, and Matsuoka M (2006). HTLV-I basic leucine zipper factor gene mRNA supports proliferation of adult T cell leukemia cells. *Proc Natl Acad Sci U S A* **103**, 720–725.
[77] Koromilas AE and Sexl V (2013). The tumor suppressor function of STAT1 in breast cancer. *JAKSTAT* **2**, e23353.
[78] Avalle L, Pensa S, Regis G, Novelli F, and Poli V (2012). STAT1 and STAT3 in tumorigenesis: A matter of balance. *JAKSTAT* **1**, 65–72.
[79] Schwinn N, Vokhminova D, Sucker A, Textor S, Striegel S, Moll I, Nausch N, Tuettenberg J, Steinle A, and Cerwenka A, et al (2009). Interferon-gamma down-regulates NKG2D ligand expression and impairs the NKG2D-mediated cytolysis of MHC class I-deficient melanoma by natural killer cells. *Int J Cancer* **124**, 1594–1604.
[80] Yeoman H and Robins RA (1988). The effect of interferon-gamma treatment of rat tumour cells on their susceptibility to natural killer cell, macrophage and cytotoxic T-cell killing. *Immunology* **63**, 291–297.
[81] Charoenthongtrakul S, Zhou Q, Shembade N, Harhaj NS, and Harhaj EW (2011). Human T cell leukemia virus type 1 Tax inhibits innate antiviral signaling via NF-kappaB-dependent induction of SOCS1. *J Virol* **85**, 6955–6962.
[82] Ko NL, Taylor JM, Bellon M, Bai XT, Shevtsov SP, Dundr M, and Nicot C (2013). PA28gamma is a novel corepressor of HTLV-1 replication and controls viral latency. *Blood* **121**, 791–800.
[83] Putz EM, Gotthardt D, Hoermann G, Csiszar A, Wirth S, Berger A, Straka E, Rigler D, Wallner B, and Jamieson AM, et al (2013). CDK8-mediated STAT1-S727 phosphorylation restrains NK cell cytotoxicity and tumor surveillance. *Cell Rep* **4**, 437–444.
[84] Jiang LJ, Zhang NN, Ding F, Li XY, Chen L, Zhang HX, Zhang W, Chen SJ, Wang ZG, and Li JM, et al (2011). RA-inducible gene-I induction augments STAT1 activation to inhibit leukemia cell proliferation. *Proc Natl Acad Sci U S A* **108**, 1897–1902.
[85] Fang Y, Zhong L, Lin M, Zhou X, Jing H, Ying M, Luo P, Yang B, and He Q (2013). MEK/ERK dependent activation of STAT1 mediates dasatinib-induced differentiation of acute myeloid leukemia. *PLoS One* **8**, e66915.
[86] Battle TE and Frank DA (2003). STAT1 mediates differentiation of chronic lymphocytic leukemia cells in response to Bryostatin 1. *Blood* **102**, 3016–3024.